

# Galvanomagnetic effects in three-band semiconductors-experiments with p-type InSb

Autor(en): **Fischer, Gaston**

Objektyp: **Article**

Zeitschrift: **Helvetica Physica Acta**

Band (Jahr): **33 (1960)**

Heft V

PDF erstellt am: **26.09.2024**

Persistenter Link: <https://doi.org/10.5169/seals-113085>

## **Nutzungsbedingungen**

Die ETH-Bibliothek ist Anbieterin der digitalisierten Zeitschriften. Sie besitzt keine Urheberrechte an den Inhalten der Zeitschriften. Die Rechte liegen in der Regel bei den Herausgebern.

Die auf der Plattform e-periodica veröffentlichten Dokumente stehen für nicht-kommerzielle Zwecke in Lehre und Forschung sowie für die private Nutzung frei zur Verfügung. Einzelne Dateien oder Ausdrucke aus diesem Angebot können zusammen mit diesen Nutzungsbedingungen und den korrekten Herkunftsbezeichnungen weitergegeben werden.

Das Veröffentlichen von Bildern in Print- und Online-Publikationen ist nur mit vorheriger Genehmigung der Rechteinhaber erlaubt. Die systematische Speicherung von Teilen des elektronischen Angebots auf anderen Servern bedarf ebenfalls des schriftlichen Einverständnisses der Rechteinhaber.

## **Haftungsausschluss**

Alle Angaben erfolgen ohne Gewähr für Vollständigkeit oder Richtigkeit. Es wird keine Haftung übernommen für Schäden durch die Verwendung von Informationen aus diesem Online-Angebot oder durch das Fehlen von Informationen. Dies gilt auch für Inhalte Dritter, die über dieses Angebot zugänglich sind.

## Galvanomagnetic Effects in Three-Band Semiconductors — Experiments with *p*-Type InSb\*)

by **Gaston Fischer**

National Research Council, Ottawa (Canada)

(3. III. 1960)

The resistivity and Hall coefficient of a *p*-type single crystal of InSb have been measured as a function of magnetic field strength and temperature. The ranges covered extend from 0 to  $\pm 8$  KOe and from 78° K to 300° K. Equations are derived for the Hall effect and the magnetoresistance which are applicable to isotropic semiconductors containing an arbitrary number of non-interacting degenerate bands, and valid for any magnetic field strength. In particular a three-band model is discussed in detail and formulae are given by which it is possible to derive values for the concentrations and mobilities of the various charge carriers from the dependence of the Hall coefficient and resistivity on the magnetic field. This model appears valid for *p*-type InSb in the extrinsic range. It predicts the presence of two kinds of hole with highly different mobilities. In the intrinsic range the model fails by giving a negative concentration of high mobility holes. An alternative model consisting of only one band of holes but taking various scattering mechanisms into account is found to be equally good at low temperatures, but also inadequate in the intrinsic range. The failure of these two models at high temperatures supports Ehrenreich's theory of predominantly polar scattering between 200° K and 500° K.

### 1. Introduction

Experimental evidence of the presence, in InSb, of two bands of holes has been recently reported<sup>1)2)</sup>. A detailed account of the situation regarding this question has been given by FREDERIKSE and HOSLER<sup>2)</sup>, and we refer the reader to their paper for extensive references. Theoretical treatments<sup>3)</sup> generally agree with an electronic structure consisting of one isotropic conduction band and two or three valence bands capable of contributing to the galvanomagnetic effects. A first valence band, observed in all experiments that depend on the electronic structure, is characterized by a high density of states and a heavy effective hole mass of about  $.18 m_0$ . The second band which is often postulated has a low density of states and a very small effective mass. Whereas everyone agrees that the light hole band is isotropic, opinions are divided about the heavy mass band. A third band with a very heavy mass of  $1.2 m_0$ , has only been

---

\*) Submitted in partial fulfilment for a Ph. D. degree at the University of Neuchâtel.

observed in cyclotron resonance experiments<sup>1</sup>), and, in agreement with theory, it is assumed to lie energetically much lower<sup>2)3)</sup>.

FREDERIKSE and HOSLER<sup>2)</sup> tried to obtain information on the band structure of InSb by performing galvanomagnetic measurements on *p*-type material below 78° K. They can explain their results with either one kind of hole and scattering predominantly through ionized impurities, or else two kinds of hole and mainly thermal scattering (scattering through thermal waves). In view of the theoretical band calculations and the evidence from cyclotron resonance experiments<sup>1)</sup> they decide in favor of the second mechanism. With the hope of obtaining a decisive choice between the two models proposed we have performed systematic galvanomagnetic measurements on a similar sample of *p*-type InSb – kindly given to us by Dr. FREDERIKSE –, but in a different temperature range. This range, between liquid nitrogen and room temperature, was so chosen as to insure an increased contribution to scattering by lattice waves. If the light mass holes postulated at low temperatures belong to a valence band, it is reasonable to assume that their number should increase with temperature; this increase need not, however, be in proportion to that of the heavy mass holes. A decrease of the number of light holes would necessitate a rather improbable temperature dependence of the band structure, or else a completely different origin would have to be attributed to these holes, for example, some kind of surface states. With the assumption of predominantly thermal scattering we would also expect holes from a valence band to show a mobility that decreases with increasing temperature. When thermal scattering alone is assumed the velocity distribution of the charge carriers in a non-degenerate semiconductor will lead to a certain variation of the resistivity and Hall coefficient with the magnetic field<sup>4)</sup>. However, these variations are relatively small and can not account for the variations observed (cf. section 4). We shall ignore this effect in the discussion of our three band model, assuming a *uniform, field independent* mobility in each band. In other words, each band is treated as a degenerate and isotropic band as in some metals. This model, which will be discussed in greater details in sections 3 to 6, appears, at first, to account extremely well for the properties observed; but when the computation is carried out completely certain inconsistencies are revealed. One finds a concentration of fast holes which decreases when temperature increases, becoming even negative above 150° K. At the same time a mobility of the fast holes is found that increases steadily with temperature, reaching values of about  $2 \times 10^5$  cm<sup>2</sup>/V. sec. While some explanation might be found for these unusual dependences on temperature, the negative charge concentration that would be required is indicative of the failure of the model in the intrinsic range.

It will be shown in section 7 that the alternative model of two bands only, with scattering by ionized impurities as well as lattice waves, is also inadequate at high temperatures. The reason for the failure of both models above 150° K probably lies in the rapid onset of a new scattering mechanism. EHRENREICH<sup>5)</sup> has shown that between 200° K and 500° K polar scattering (i. e. scattering through longitudinal optical modes of vibration) is predominant. EHRENREICH's calculations nevertheless support a three-band model.

Hall effect and conductivity of InSb as a function of magnetic field have been measured by many investigators, but the first systematic description of a model consisting of three bands was given by WILLARDSON<sup>6)</sup> in an investigation of *p*-type germanium. A fine structure analysis of a number of *p*-type semiconductors has been carried out by BEER<sup>7)</sup> and BEER and WILLARDSON<sup>8)</sup>. Their experiments on germanium, silicon, diamond and aluminum antimonide reveal maxima and minima which they can explain with a complex scattering mechanism and the presence of two kinds of hole. To carry out such an analysis requires the help of big computing devices.

## 2. Experimental Procedure

From a *p*-type single crystal of InSb a sample appropriate to the measurements was ground to size with fine emery paper since the material was too brittle to be cut with a diamond saw. Orientation and dimensions of this sample are given in Table I. The sample was mounted in the same

Table I  
Dimensions in mm and Orientation of the Single Crystal Sample

	$l$	$\delta$	$d$	$w$	$t$
Dimension . . .	16	16	4.80	3.86	1.14
Orientation. . .	(100)	(100)	(100)	9° off (010)	9° off (001)
$l$ = length of sample; $\delta$ = distance between current leads; $d$ = distance between potential leads; $w$ = width; $t$ = thickness					

way as described in a previous paper<sup>9)</sup>, but the current leads were soldered onto the whole areas of the smallest sample faces in order to ensure a more regular potential distribution. The soldering was done with indium, platinizing solution being used as a flux. The geometry of the sample is a factor which can substantially affect galvanomagnetic measurements. The work of LIPPMAN and KUERT<sup>10)</sup> indicates that with the dimensions of our sample the Hall constant should not be affected by more than one percent, while a rather greater alteration must be expected in the magnetoresistance, particularly at higher fields. The technique of pressure

contacts for the potential and Hall voltage leads<sup>9)</sup> provides very small areas of contact to the sample, along lines of constant potential, and should thus cause only a very small perturbation.

Our measurements were consistently performed between  $-8$  KOe and  $+8$  KOe. No significant asymmetry in the magnetoresistance or Hall effect was found. The largest difference between the positive and negative branches of the resistivity curves was only 2%; it was systematically in one direction below  $190^\circ\text{K}$  and in the other direction above, being greatest at the highest temperatures. Except in the vicinity of the sign reversal,

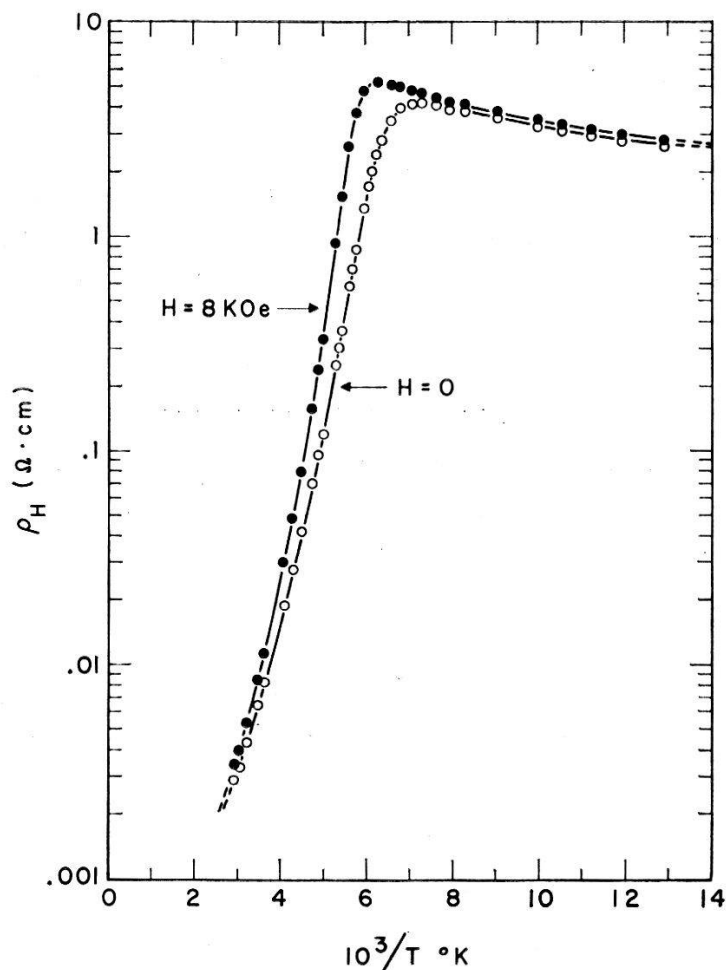


Fig. 1

Resistivity versus temperature of a single crystal of InSb at magnetic fields of 0 and 8 KOe

at  $150^\circ\text{K}$ , the Hall coefficient was found to be perfectly symmetrical with the magnetic field  $H$ . Where it changes sign the Hall coefficient is so sensitive to any change in the concentration of impurities that an appreciable systematic asymmetry must be expected. The range of temperature over which this occurs is narrow, from  $150^\circ\text{K}$  to  $170^\circ\text{K}$ , and if one takes averages between the positive and negative field readings one may expect

to obtain reasonable results. For the sake of consistency this averaging procedure was carried out with all measurements of the resistivity,  $\rho_H$ , and the Hall voltage,  $V_H$ . The almost perfect symmetry observed justifies the technique of pressure-contacts, and indicates a high degree of homogeneity of the sample<sup>11</sup>).

The magnetic field was calibrated with a nuclear magnetic resonance spectrometer. Care was taken to identify the whole hysteresis cycle; when resetting a certain field the current was first increased well into the saturation range and then monotonically decreased to the appropriate value. The accuracy in resetting a given field was of the order of  $\pm 10$  Oersteds.

Figs. 1 and 2 reproduce the temperature dependence of the resistivity and Hall effect in the fields  $H = 0$  and  $H = 8$  KOe. With these properties we can obtain a rough estimate of the purity of our sample by assuming that only one kind of hole is present at liquid nitrogen temperature and by simply equating the number  $n_2$  of these holes to the number  $N$

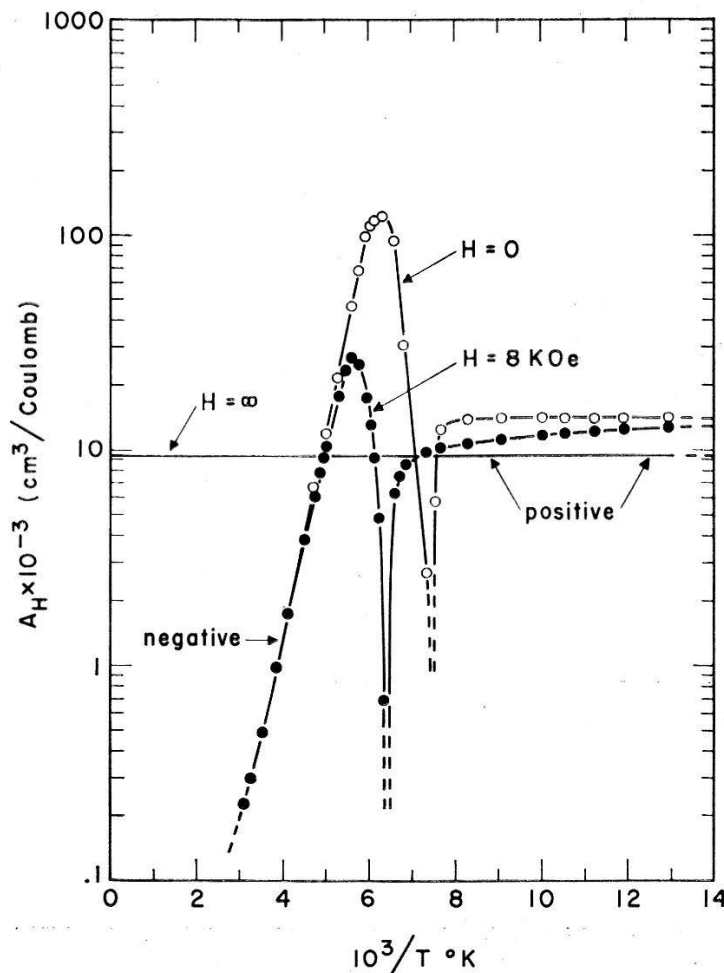


Fig. 2

Hall coefficient versus temperature of a single crystal of InSb at magnetic fields of 0, 8 KOe and  $\infty$

of acceptors per  $\text{cm}^3$ . We shall use the approximate equations (2.1) and (2.2) to perform this computation (the symbols are defined in the next section).

$$\rho_0(77^\circ \text{K}) = \frac{1}{n_2 e b_2} = 2.6 \Omega \text{ cm} \quad (2.1)$$

$$A_0(77^\circ \text{K}) = \frac{1}{n_2 e} = 14 \times 10^3 \text{ cm}^3/\text{Coulomb} \quad (2.2)$$

From (2.2) one readily obtains

$$n_2 = N = \frac{1}{e A_0} = 4.5 \times 10^{14} \text{ cm}^{-3} \quad (2.3)$$

and with (2.1) one can get  $b_2$  as

$$b_2 = \frac{1}{n_2 e \rho_0} = 5.4 \times 10^3 \text{ cm}^2/\text{V. sec} \quad (2.4)$$

### 3. Equations of the Three-Band Semiconductor

We shall follow CHAMBERS<sup>12)</sup> to derive the resistivity  $\rho_H$ , and Hall coefficient,  $A_H$ , of a three-band semiconductor. Let us define

$$t_i = A_{Hi} \sigma_i H \quad (3.1)$$

and

$$\varnothing_i = \frac{\sigma_i}{1 + t_i^2} \quad (3.2)$$

where  $\sigma_i$  and  $A_{Hi}$  are the conductivity and Hall coefficient of the *separate* band  $i$ . Chambers has shown that for any number  $n$  of *non interacting* and *isotropic* bands one can write

$$\varnothing = \sum_{i=1}^n \varnothing_i \quad (3.3)$$

and

$$\varnothing t = \sum_{i=1}^n \varnothing_i t_i \quad (3.4)$$

with  $\varnothing$  and  $t$  related to the conductivity  $\sigma$  and the Hall coefficient  $A_H$  of the complete system:

$$t = A_H \sigma H \quad (3.5)$$

$$\varnothing = \frac{\sigma}{1 + t^2} \quad (3.6)$$

It is worth noting that the field  $H$  is proportional to every  $t_i$  and to  $t$ . If we assume in each band  $i$  a concentration of carriers  $n_i$  and a *uniform mobility*  $b_i$ , we can write

$$i = n_i e b_i \dots \quad (i = 1, 2, \dots n) \quad (3.7)$$

and

$$A_{Hi} = \frac{1}{n_i e c} \quad (3.8)$$

Expressions (3.7) and (3.8) are given with the convention that  $e$  is taken positive, electrons are attributed negative  $n_i$  and  $b_i$ 's, and holes are given positive  $n_i$  and  $b_i$ 's.

From (3.5) and (3.6) it is now possible to calculate the resistivity  $\rho_H = 1/\sigma$  and the Hall coefficient  $A_H$  of the complete system:

$$\rho_H = \frac{1}{e} \cdot \frac{\sum_i n_i b_i \left\{ \prod_{j \neq i} (1 + b_j^2 H^2) \right\}}{\sum_i n_i^2 b_i^2 \left\{ \prod_j (1 + b_j^2 H^2) \right\} + 2 \sum_{i,k} n_i n_k b_i b_k (1 + b_i b_k H^2) \left\{ \prod_{j \neq i,k} (1 + b_j^2 H^2) \right\}} \quad (3.9)$$

$$A_H = \frac{1}{ec} \cdot \frac{\sum_i n_i b_i^2 \left\{ \prod_j (1 + b_j^2 H^2) \right\}}{\sum_i n_i^2 b_i^2 \left\{ \prod_j (1 + b_j^2 H^2) \right\} + 2 \sum_{i,k} n_i n_k b_i b_k (1 + b_i b_k H^2) \left\{ \prod_k (1 + b_j^2 H^2) \right\}} \quad (3.10)$$

It is seen at once that both formulae are quotients of two even polynomials of order  $2(n-1)$  in  $H$ , where  $n$  is the number of bands. The polynomials of the two denominators are identical.

We shall now consider a three-band model. Expressing everything in laboratory units<sup>9</sup>), and writing  $(10^{-8} H)^2 = x$ , one can reduce (3.9) and (3.10) to the following simple formulae

$$\rho_H = \frac{1}{e} \cdot \frac{A + Bx + Lx^2}{A^2 + Dx + Mx^2} \quad (3.11)$$

$$A_H = \frac{1}{e} \cdot \frac{E + Fx + Nx^2}{A^2 + Dx + Mx^2} \quad (3.12)$$

For the various parameters of these formulae one obtains:

$$A = n_1 b_1 + n_2 b_2 + n_3 b_3 \quad (3.13)$$

$$B = n_1 b_1 (b_2^2 + b_3^2) + n_2 b_2 (b_1^2 + b_3^2) + n_3 b_3 (b_1^2 + b_2^2) \quad (3.14)$$

$$L = (n_1 b_2 b_3 + n_2 b_1 b_3 + n_3 b_1 b_2) b_1 b_2 b_3 \quad (3.15)$$

$$D = (n_1 + n_2)^2 b_1^2 b_2^2 + (n_1 + n_3)^2 b_1^2 b_3^2 + (n_2 + n_3)^2 b_2^2 b_3^2 + 2 n_1 n_2 b_1 b_2 b_3^2 + 2 n_1 n_3 b_1 b_3 b_2^2 + 2 n_2 n_3 b_2 b_3 b_1^2 \quad (3.16)$$

$$M = (n_1 + n_2 + n_3)^2 b_1^2 b_2^2 b_3^2 \quad (3.17)$$

$$E = n_1 b_1^2 + n_2 b_2^2 + n_3 b_3^2 \quad (3.18)$$

$$F = n_1 b_1^2 (b_2^2 + b_3^2) + n_2 b_2^2 (b_1^2 + b_3^2) + n_3 b_3^2 (b_1^2 + b_2^2) \quad (3.19)$$

$$N = (n_1 + n_2 + n_3) b_1^2 b_2^2 b_3^2 \quad (3.20)$$



The parameter  $\Lambda$ , defined in previous papers<sup>9)13)</sup>, is not explicitly independent of the magnetic field  $H$ , as it is for the two-band model.

$$\Lambda \equiv \left( \frac{A_H - A_0}{A_0} \right) / \left( \frac{\rho_H - \rho_0}{\rho_0} \right) = \frac{A^2 F - ED + (A^2 N - EM)x}{E(AB - D) + E(AL - M)x} \quad (3.21)$$

If the coefficients of the above expression for  $\Lambda$  are independent of  $H$ , then  $\Lambda$  cannot become an extremum at fields other than  $H = 0$  or  $H = \infty$ .

We shall now discuss the properties of our three-band model, with the additional assumption that all charge carrier concentrations and mobilities are independent of the magnetic field.  $n_1$  and  $b_1$  are attributed to electrons and are thus negative.  $n_2$  and  $b_2$  refer to the heavy holes,  $n_3$  and  $b_3$  refer to the light holes, and these four parameters are therefore positive. The light holes are assumed to have a higher mobility, and they belong to a band with a lower density of states; one can then write the inequalities

$$n_2 \gg n_3 \quad (3.22)$$

$$b_2 < b_3 \quad (3.23)$$

We shall also assume that the mobility  $b_1$  of the electrons is larger than the mobility  $b_2$  of the heavy holes. Thus

$$-b_1, b_3 > b_2 > 0 \quad (3.24)$$

In principle it should be possible to solve the system (3.13) to (3.20), obtaining first two relations between the eight equations; this would reduce the system to only six equations. Then secondly, solve for the six physical parameters  $n_1$  to  $b_3$ . However, the complexity of the system is so great that it seems appropriate to try first to determine the general and particular characters of our model for the two kinds of material,  $p$ - and  $n$ -type.

#### 4. Discussion of a $p$ -type model of InSb

We shall speak of a  $p$ -type semiconductor when, for every temperature,

$$\mathfrak{N} = n_1 + n_2 + n_3 > 0 \quad (4.1)$$

If all acceptors and donors are fully ionized,  $\mathfrak{N}$  will be a constant; this will happen at all temperatures where  $kT$  is much greater than the ionization energy of the acceptors and donors. We can check if  $\mathfrak{N}$  is a constant in our sample over the temperature range of our measurements, since

$$A_\infty \equiv A_{H \rightarrow \infty} = \frac{1}{e} \cdot \frac{N}{M} = \frac{1}{e\mathfrak{N}} \quad (4.2)$$

Figure 3 strongly suggests that  $A_\infty$ , and therefore also  $\mathfrak{N}$ , are constant. Equation (4.2) is of a very general character; if we write  $\mathfrak{N} = \sum_{i=1}^n n_i$ , then for a system of any number  $n$  of separate bands,

$$A_\infty = \frac{1}{e\mathfrak{N}_\infty} \quad (4.3)$$

where  $\infty$ , the subscript of  $\mathfrak{N}$ , means that any change in the concentrations  $n_i$  due to the magnetic field has to be taken into account. This result is no different from the conclusions which can be drawn from a one- or two-band model, and the observed constancy of  $A_\infty$  with temperature does not provide evidence in favor of any particular number of bands. It is, nevertheless, interesting to note the good convergence of all the curves of Figure 3 towards a constant, mobility independent  $A_\infty$ , particularly if we remember that at finite fields the Hall coefficient can depend very much on the mobilities.

Let us consider the ratio

$$\frac{A_0}{A_\infty} = \frac{EM}{A^2N} = \frac{n_1 b_1^2 + n_2 b_2^2 + n_3 b_3^2}{(n_1 b_1 + n_2 b_2 + n_3 b_3)^2} \cdot \mathfrak{N} \quad (4.4)$$

$$\frac{A_0}{A_\infty} = \frac{n_1 \mathfrak{N} b_1^2 + n_2 \mathfrak{N} b_2^2 + n_3 \mathfrak{N} b_3^2}{(n_1 b_1 + n_2 b_2 + n_3 b_3)^2} \quad (4.5)$$

At very low temperatures  $n_1$  vanishes (our sample is free of donors, cf. Table III), and  $\mathfrak{N}$  simply equals  $n_2 + n_3$ . Because of (3.23) it is then possible to have

$$\frac{A_0}{A_\infty} > 1 \quad (4.6)$$

This result is very important, since it cannot be obtained with a two-band model of carriers with opposite charges. A two-band semiconductor with carriers of opposite charges requires condition

$$\frac{A_0}{A_\infty} \leq 1 \quad (4.7)$$

Our present measurements on single crystalline InSb, as well as unpublished ones on a polycrystalline sample, indicate that condition (4.6) is fulfilled and give support to a model of at least two kinds of hole. At this point it can be argued that with the consideration of thermal scattering our findings could be explained within the framework of a two-band model. WILSON<sup>4)</sup> has shown that owing to the thermal spread of the velocities a semiconductor will require

$$\frac{A_0}{A_\infty} \leq \frac{3\pi}{8} = 1.18 \quad (4.8)$$

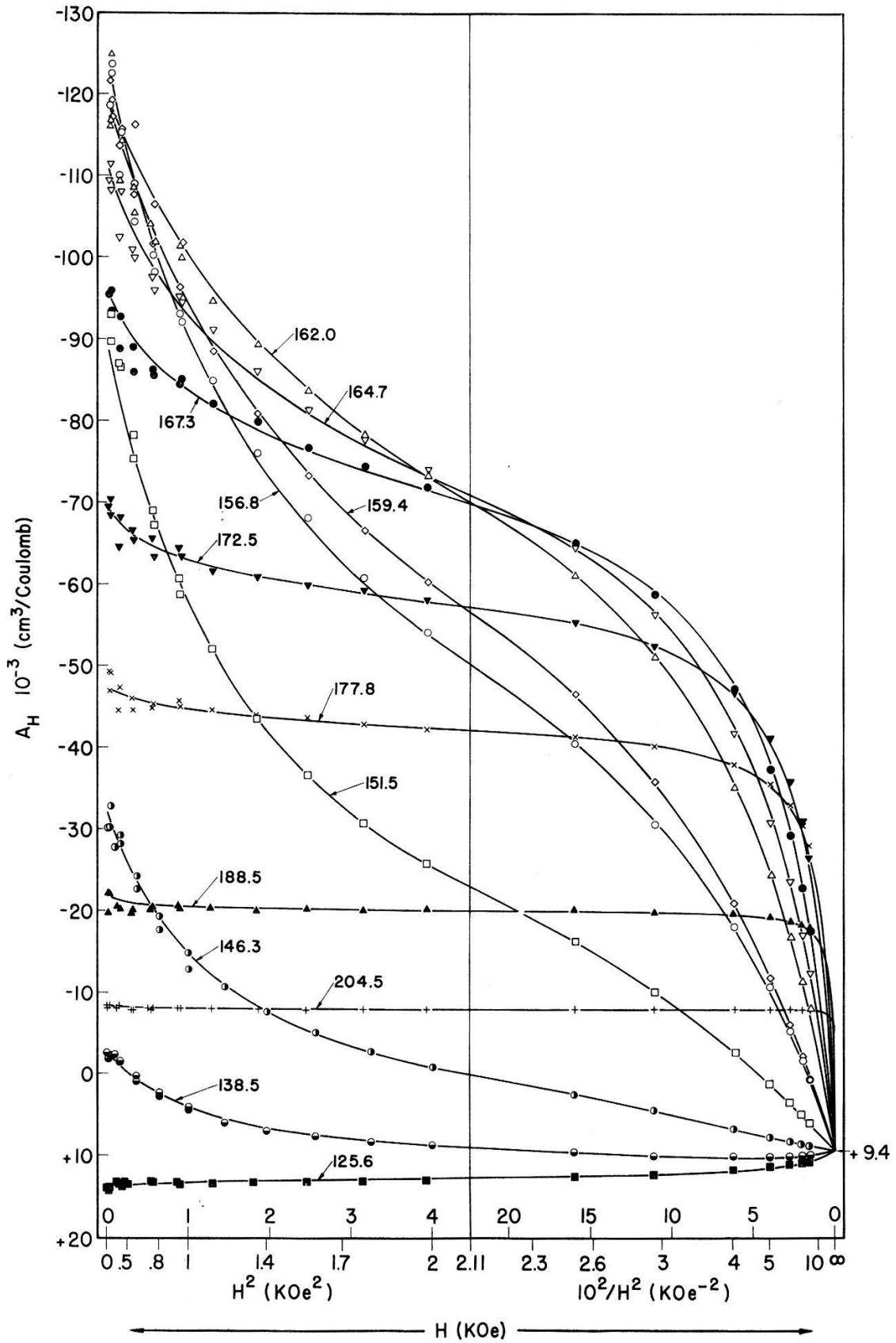


Fig. 3

Our measurements give, however, a definitely larger ratio. According to Figure 3 we have

$$\frac{A_0}{A_\infty} = \frac{13,900}{9,400} = 1.48 \quad (4.9)$$

and the value obtained with a polycrystal is about 1.35. These results, therefore, are easier to explain with two kinds of hole than with a thermal spread of velocities. HROSTOWSKI *et al.*<sup>14)</sup> also observed a ratio greater than 1.18.

It can be seen that within a certain range of temperatures the same ratio  $A_0/A_\infty$  can obtain negative values of a magnitude several times greater than unity. This prediction, which is well realized in our measurements in the range of 145°K to 195°K (cf. Fig. 2), is only typical of semiconductors with carriers of opposite signs.

There is, however, a property which can only occur in semiconductors with uniform mobilities in each band when at least three kinds of carrier are present; this is an extremum of  $A_H$  for fields different from zero or infinity. Considering condition (4.10),

$$\frac{\partial A_H}{\partial x} = 0 \quad (4.10)$$

we obtain

$$x^2 (ND - FM) + 2x (NA^2 - ME) + A^2 F - ED = 0 \quad (4.11)$$

and look for positive roots of this equation. Let us start by rewriting equation (4.11) in the simpler manner

$$ax^2 + 2bx + c = 0 \quad (4.12)$$

A careful study will show that at the lowest temperatures all three coefficients  $a$ ,  $b$  and  $c$  of this equation are negative. One by one these coefficients change sign in going through zero. First to change is  $c$ , then  $b$  and finally  $a$ . In the range where  $a$  and  $c$  have opposite signs there will be a maximum of  $A_H$  versus  $H$ . Outside this range there will be no extremum (cf. Table II and Fig. 3). No such extremal values are possible with a similar two-band model. The present three-band model could thus explain the maximum in the Hall coefficient observed by HOWARTH *et al.*<sup>15)</sup> as well as in our present (Fig. 3) and previous<sup>9)</sup> papers.

Fig. 3

Hall coefficient versus magnetic field of a single crystal of InSb at various temperatures. The points are experimental and the curves are calculated. Note the change of scale on the abscissa to bring out the important features near  $H = 0$  and  $H = \infty$ . An appropriate choice of scales for the two halves of the diagram will ensure continuous derivatives. The scales on the abscissa are the same as in Fig. 4, and the reader is referred to that figure for greater clarity.

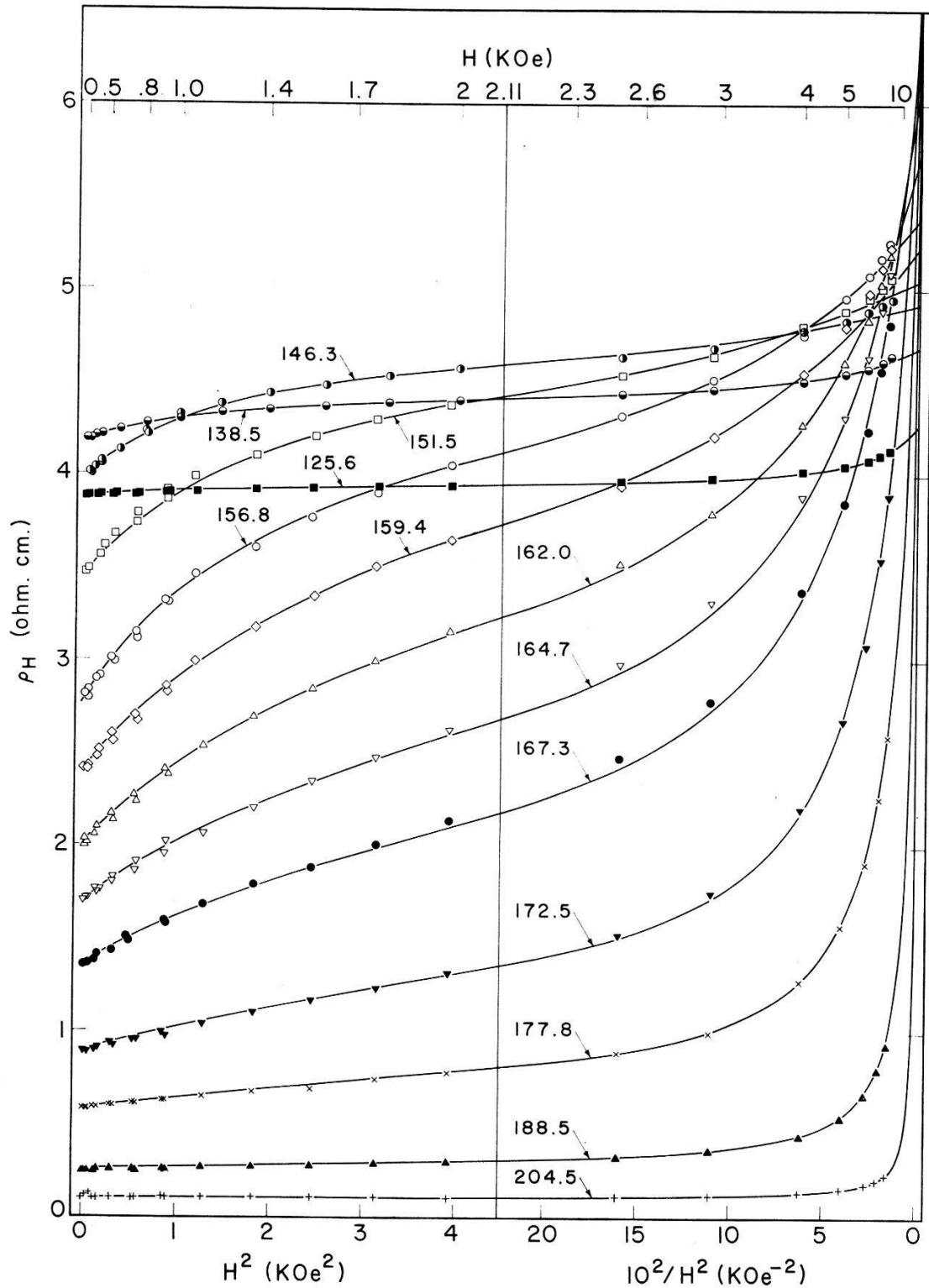


Fig. 4

Resistivity versus magnetic field of a single crystal of InSb at various temperatures. The points are experimental and the curves are calculated. Note the change of scale as in Fig. 3

We have now gathered sufficient information to predict the general behaviour of  $A_H$  versus magnetic field  $H$  and temperature for a  $p$ -type semiconductor having two types of positive charge carrier. In Figure 3

calculated curves are displayed which are of the type (3.12) and also fit, as well as possible, our own measurements. There is good agreement.

A discussion of the resistivity  $\rho_H$  similar to the above discussion of  $A_H$  is not of great interest, since there is no essential difference between the predictions for  $\rho_H$  of a two- and three-band model. The differences are only quantitative. Figure 4 gives calculated curves according to (3.11) and our measured points. The denominator of the calculated  $\rho_H$  curves is the same as that of the Hall coefficient curves (Fig. 3), as required by the theory. The numerator ignores the two unknown relations which must exist between all the parameters involved in the formulae (3.11) and (3.12) and was simply chosen to give a satisfactory fit.

Table II and Figures 5 and 6 give the values chosen for the parameters appearing in formulae (3.11) and (3.12), at the various temperatures of our measurements.

In section 6 a complete solution of the system of equations (2.13) to (2.20) is given, and a computation of the charge carrier concentrations and mobilities is carried out.

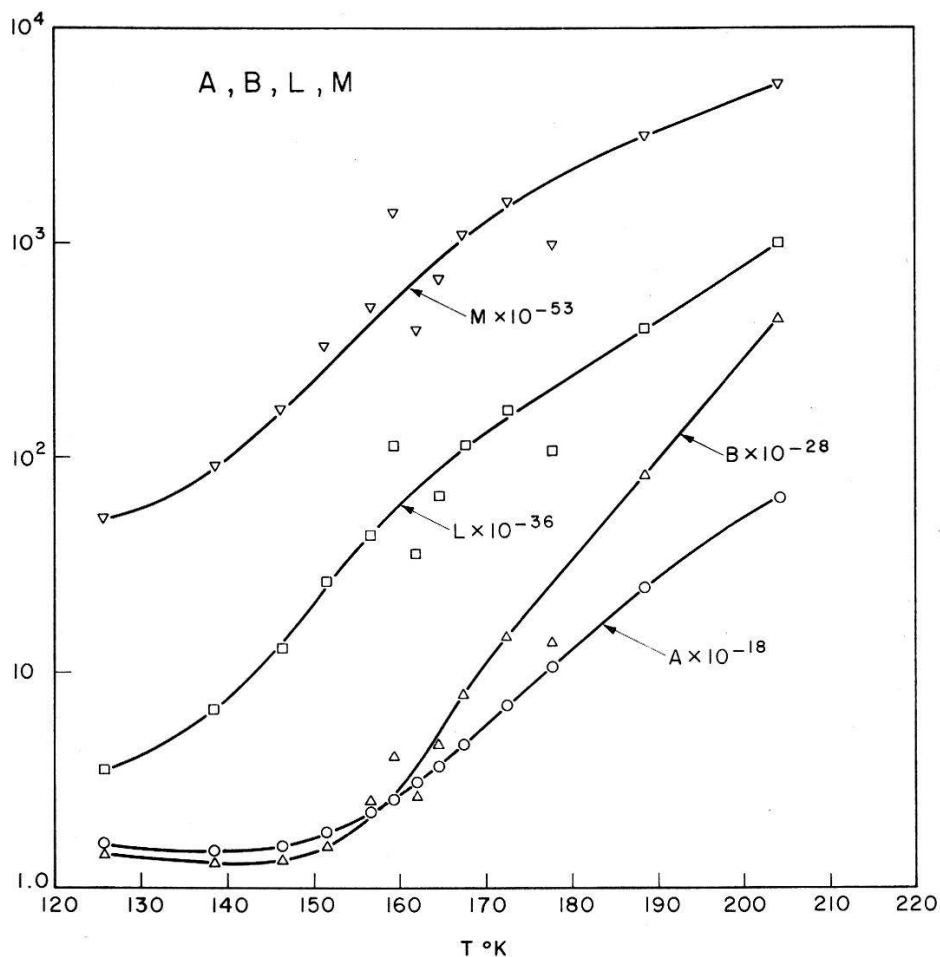


Fig. 5

Parameters  $A$ ,  $B$ ,  $L$ , and  $M$  of formulae (2.11) and (2.12) versus temperature.

Table II

Coefficients  $A$ ,  $B$ ,  $D$ ,  $E$ ,  $F$ ,  $L$ ,  $M$ , and  $N$  of formulae (2.11) and (2.12) as derived from the experiments. Calculated values of  $B$  and  $L$  are obtained in a manner described in Section 5. The coefficients  $a$ ,  $b$ , and  $c$  are defined in formulae (3.12) and (3.11)

$T^\circ \text{K}$	125.6	138.5	146.3	151.5	156.8	159.4	162.0	164.7	167.3	172.5	177.8	188.5	204.5
$A \cdot 10^{-18}$	1.611	1.491	1.564	1.800	2.232	2.593	3.100	3.668	4.630	7.078	10.74	24.80	65.10
$B \cdot 10^{-28}$	1.435	1.297	1.349	1.575	2.567	4.111	2.713	4.677	7.963	14.85	13.98	83.95	443.6
$B \cdot 10^{-28}$ (calc.)	1.424	1.285	1.306	1.559	1.73	3.74	1.83	3.59	6.57	12.81	12.43	80.92	456.3
$D \cdot 10^{-46}$	2.284	1.838	1.816	2.268	4.215	8.743	5.766	13.63	30.33	91.68	133.1	2,051	28,640
$E \cdot 10^{-21}$	+ 5.777	-0.9593	-12.53	-45.87	-98.16	-127.5	-183.3	-238.4	-328.2	-556.0	-870.7	-2,146	- 5,635
$F \cdot 10^{-31}$	+ 4.645	+ 3.552	+ 1.761	- 8.284	- 41.96	- 127.5	- 69.38	- 174.0	- 379.4	- 889.5	- 912.8	- 6,629	- 36,610
$L \cdot 10^{-36}$	3.560	6.680	12.87	26.20	42.97	112.8	35.34	66.02	111.1	164.6	106.9	400.0	985.8
$L \cdot 10^{-36}$ (calc.)	3.529	6.468	12.16	23.29	32.51	107.4	28.5	58.9	103.3	152.5	103.0	387.8	1,092
$M \cdot 10^{-54}$	5.191	8.892	16.31	32.40	49.82	134.5	38.44	67.27	107.2	151.8	96.11	307.5	529.8
$N \cdot 10^{-39}$	7.807	13.37	24.53	48.73	74.93	202.3	57.81	101.2	161.2	228.3	144.5	462.5	796.8
$a \cdot 10^{-85}$	- 6.281	- 7.010	+ 15.82	+ 378.9	2,406	18,910	3,000	13,080	45,560	156,000	96,160	2,987,000	42.21 $\cdot 10^6$
$b \cdot 10^{-75}$	- 9.727	+ 38.25	+ 264.4	+ 1,644	5,264	18,510	7,602	17,400	38,640	95,840	10.04 $\cdot 10^4$	94.44 $\cdot 10^4$	63.62 $\cdot 10^5$
$c \cdot 10^{-67}$	- 1.139	+ 9.660	+ 27.06	+ 77.19	204.7	257.2	390.2	908.4	1,821	6,412	45,243	32.43 $\cdot 10^4$	85.24 $\cdot 10^5$

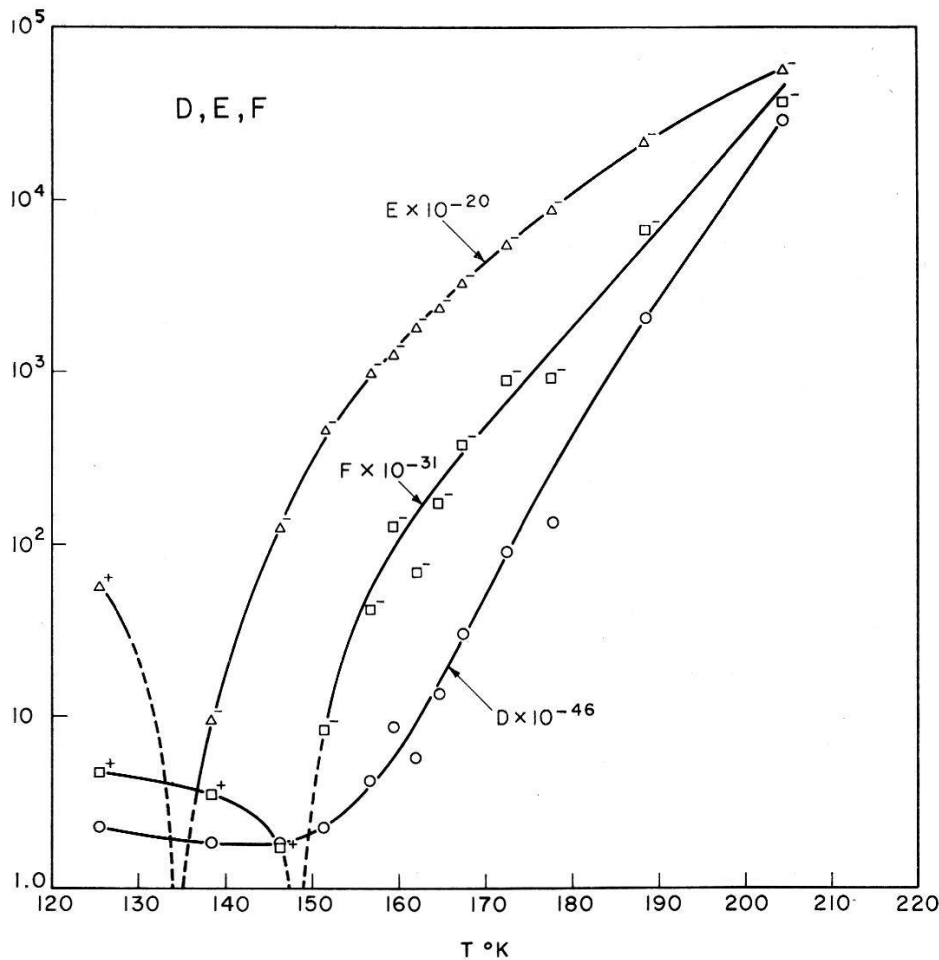


Fig. 6

Parameters  $D$ ,  $E$ , and  $F$  of formulae (2.11) and (2.12) versus temperature

### 5. Discussion of $n$ -type InSb

Although we have done no experiments with  $n$ -type material, we shall discuss briefly the properties to be expected from  $n$ -type InSb, when again (3.24) is valid.

$n$ -type semiconductors can be defined by the condition

$$\mathfrak{N} = n_1 + n_2 + n_3 < 0 \tag{5.1}$$

Assuming that above a certain temperature all donors and acceptors are fully ionized, and that the magnetic field has no effect on the  $n_i$ 's, one would again expect  $A_\infty$  to be a constant

$$A_\infty = \frac{1}{e\mathfrak{N}_\infty} \tag{5.2}$$

Considering the ratio  $A_0/A_\infty$  as defined by (4.5) one sees at once that for an  $n$ -type semiconductor with only one kind of electron and satisfying (3.22) and (3.24) one always has

$$0 < \frac{A_0}{A_\infty} \leq 1 \tag{5.3}$$



This result is independent of the number of bands of holes. Again it must be said that this condition may be slightly violated because of the thermal velocity spread, to the extent shown by WILSON<sup>4</sup>). One could thus replace (5.3) by

$$0 < \frac{A_0}{A_\infty} \leq \frac{3\pi}{8} = 1.18 \quad (5.4)$$

In both inequalities (5.3) and (5.4) the equality sign can only occur at low temperatures.  $A_0$  is negative like  $A_\infty$ , and because of (3.24) never changes sign with temperature; its magnitude will decrease when the temperature increases, unless extremely improbable temperature variations of the mobilities take place.

We shall now look for possible extrema of  $A_H$  versus  $H$ . Again (4.10) will give us (4.11) which we write more simply as (4.12). One can see that  $a$ ,  $b$  and  $c$  are always negative, and as a result there should be no maxima or minima. It must be noted, however, that unlike  $p$ -type InSb for which  $A_H$  can vary over an extremely large range of values, extending from positive values larger than  $A_\infty$  to negative values of a magnitude several times larger than  $A_\infty$ ,  $n$ -type InSb only allows  $A_H$  values in the range given by (5.3) or (5.4). Mobility and charge carrier concentration changes, which are difficult to observe in  $p$ -type InSb because of the large variations of  $A_H$ , may be more readily detected in  $n$ -type InSb. It is therefore particularly interesting that a number of recent experiments with  $n$ -type InSb have shown features which are not as yet wholly understood.

FREDERIKSE and HOSLER<sup>16</sup>) have observed several maxima and minima of the Hall coefficient in  $n$ -type InSb at 78° K and below; they give no explanation of this behaviour. BATE, WILLARDSON and BEER<sup>17</sup>) have also observed a minimum of  $A_H$  versus  $H$  in  $n$ -type InSb at temperatures of 55° K to 195° K, for which they too could give no explanation, although they considered complex scattering mechanisms.

## 6. Computation of the Charge Carrier Concentrations and Mobilities

The system of eight equations (3.13) to (3.20) could first have been reduced to only six independent relations, since there are only six unknowns. However, this seemed too complicated and we tried to obtain a solution from a set of any six equations. The remaining two were then used to check the consistency of the experimental parameters with the theory. The mathematical method which will be described in Appendix I has been chosen because of two important advantages. First of all it is algebraically quite simple. Secondly, it does not make use of  $B$  and  $L$  which are determined from the magnetoresistance measurements. As has been seen in section 2, magnetoresistance is more affected than Hall effect by sample geometry, and it is advisable to discard those parameters

which have been derived from the dependence on the magnetic field of the sample resistance. With the computed carrier concentrations one can in turn obtain calculated values of  $B$  and  $L$ . It is interesting to compare these calculated values with those obtained from the experiments (Table II). The agreement is very good and indicates that all the experimental parameters obtained are highly compatible with each other within the theory presented; it is also indicative that the geometrical effect produced only small perturbations.

Table III and Figures 7 to 12 give the computed charge carrier concentrations,  $n_i$ , and the mobilities,  $b_i$ , versus the temperature  $T$ . With the exception of  $n_3$  and  $b_3$  the values obtained appear to be very reasonable, not too scattered, and with a plausible temperature dependence. The values obtained for  $n_3$  and  $b_3$  are reasonable only below  $150^\circ\text{K}$ ; above

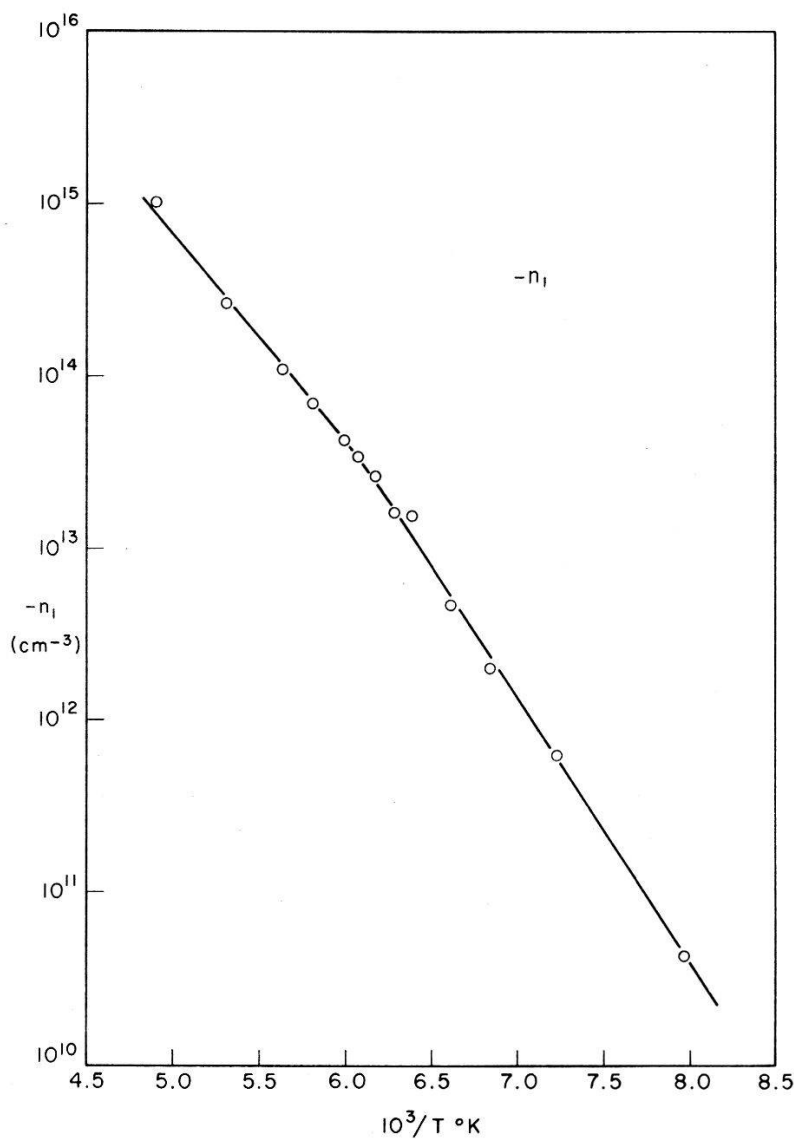


Fig. 7

Concentration of electrons versus temperature

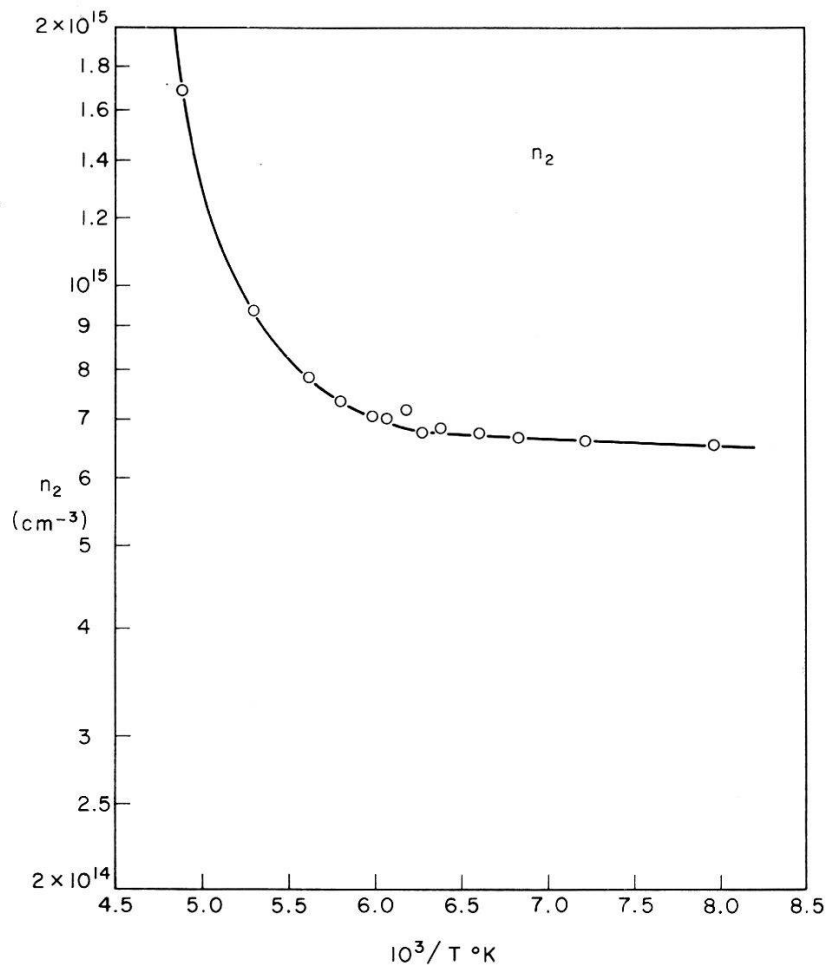


Fig. 8

Concentration of «slow» holes versus temperature

that temperature  $n_3$  becomes negative, while  $b_3$  starts increasing towards rather high values. The negative values of  $n_3$  seem to be a physically impossible result, since by definition (section 3) we would always expect the same signs for  $n_i$  and its corresponding  $b_i$ . The success of our model below  $150^\circ\text{K}$  was to be expected, since it is in that temperature range that features most characteristic of a three carrier model appear to be followed by our sample.

Figure 13 is a graph of  $\log [-n_1(n_2 + n_3)/T^3]$  versus  $1/T$ . Simple activation theories predict this relation to be linear, with a slope yielding the energy gap at the absolute zero. We obtain  $\Delta E = 0.27\text{ eV}$ , a value slightly higher than the recent quotation of  $0.25\text{ eV}^{18}$ .

### 7. Discussion of an Alternative Model

A model consisting of two degenerate bands, one of electrons and one of holes, has proved inadequate to explain the field dependence observed. Only in the narrow range from  $150^\circ\text{K}$  to  $160^\circ\text{K}$  does it happen that our experimental curves  $A_H$  and  $\rho_H$  can be represented almost equally well

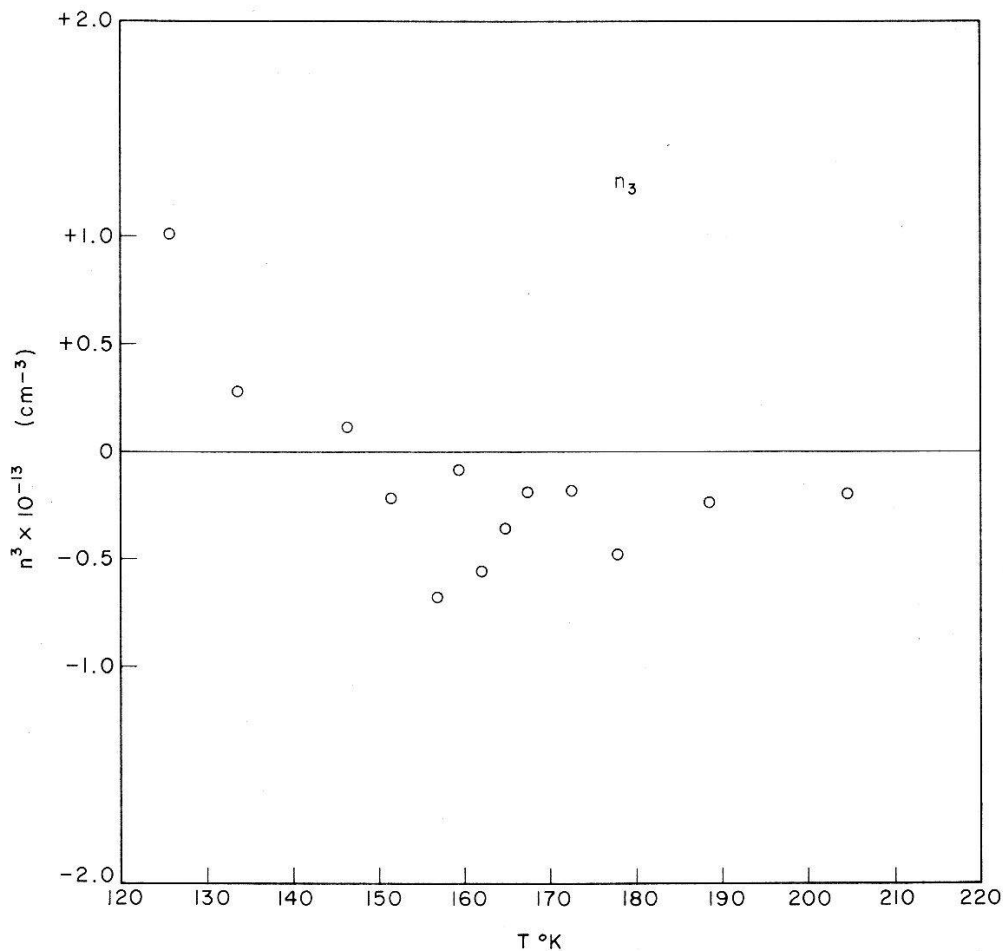


Fig. 9  
Concentration of «fast» holes versus temperature

by a two band model of properties similar to the three-band model discussed so far. To check if taking the thermal spread of velocities and the scattering by ionized impurities into account would improve the situation it is convenient to consider the parameter  $\Lambda$  defined elsewhere<sup>9)13)</sup>. We recall that, under reasonable simplifying conditions,  $\Lambda$  should obey the following relation:

$$\Lambda(H=0) = \left\{ \frac{\Lambda(H=\infty) + (1-\alpha)/(Q-1)}{1 + (1-\gamma)/(Q-1)} \right\} \cdot \frac{\gamma}{\alpha} \quad (7.1)$$

(we refer to reference 9) for the definition of the symbols) and we have erroneously stated<sup>9)</sup> that the following inequality follows:

$$\Lambda(0) \geq \Lambda(\infty) \quad (7.2)$$

(7.2) is correct only when  $\Lambda(\infty)$  satisfies the very restrictive condition (7.3):

$$\Lambda(\infty) \left\{ \frac{Q-1}{Q-\gamma} - \frac{\alpha}{\gamma} \right\} \geq -\frac{1-\alpha}{Q-\gamma} \quad (7.3)$$

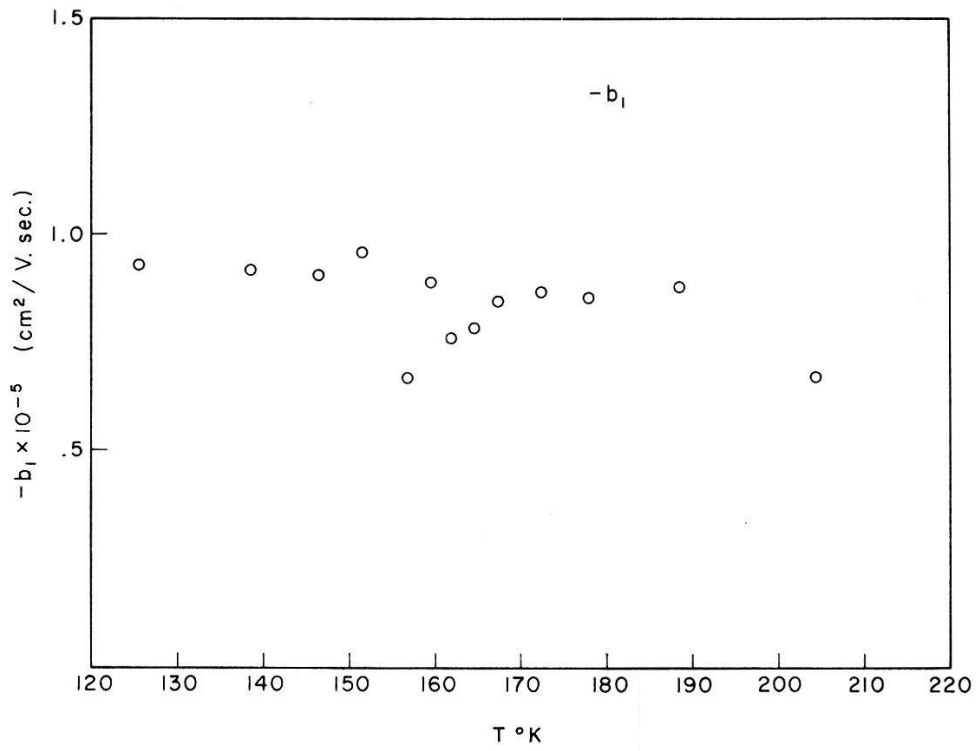


Fig. 10  
Mobility of electrons versus temperature

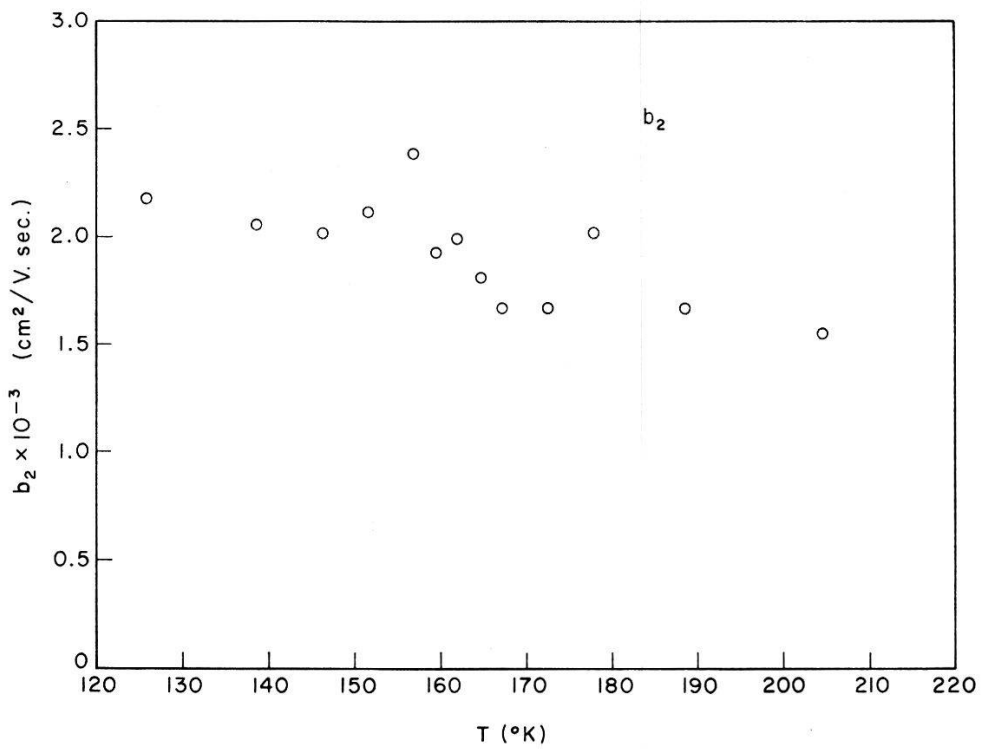


Fig. 11  
Mobility of «slow» holes versus temperature

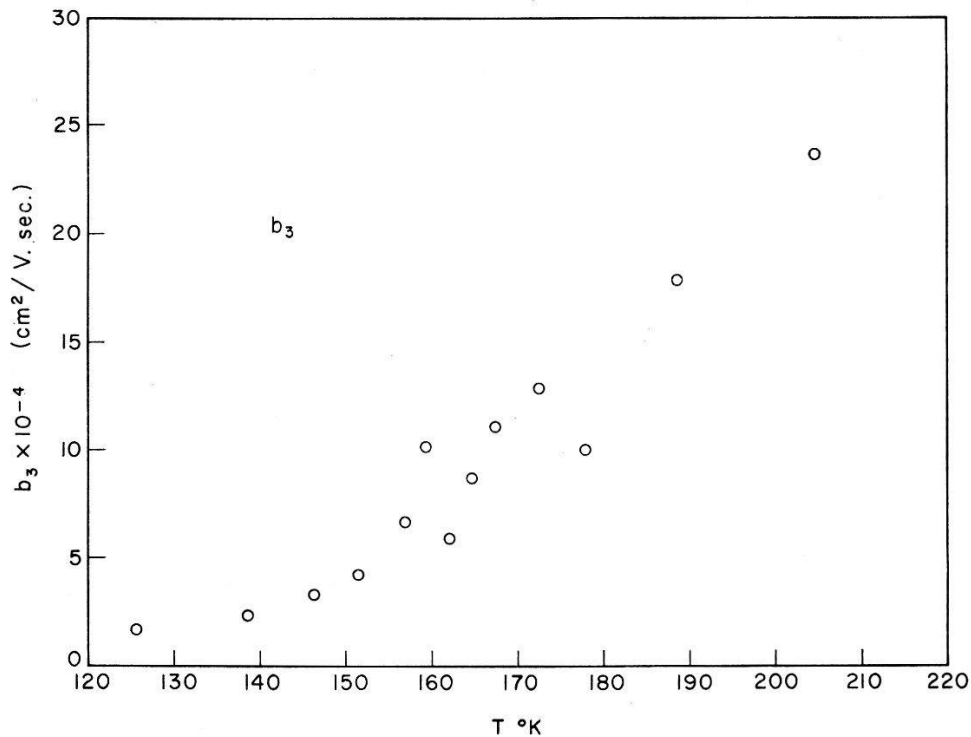


Fig. 12  
Mobility of «fast» holes versus temperature

This condition is not satisfied in *p*-type InSb and it is seen in Figure 14 that one has throughout  $\Lambda(0) < \Lambda(\infty)$ .

Depending on the degree of degeneracy and on the relative amounts of scattering by lattice waves and ionized impurities  $\alpha$  and  $\gamma$  should be comprised between the following limits<sup>4)</sup>

$$.5 \leq \alpha \leq 1 \quad (7.4)$$

$$2 \geq \gamma \geq 1 \quad (7.5)$$

Now  $Q$ ,  $\Lambda(0)$  and  $\Lambda(\infty)$  can be derived from our measurements, using functions (3.11) and (3.12), and the parameters of Table II. We know that these calculated functions fit the measurements very well and it can be seen in Figure 14 that the values so obtained are likely extrapolations of the experimental points at finite magnetic fields. Assuming for  $\alpha$  the three values .5; .849; and 1 one can calculate  $\gamma$ . If the  $\gamma$  values obtained satisfy (7.5) we might conclude that our alternative model is valid for *p*-type InSb. As can be seen from Table IV and Figure 15 this does not occur for all temperatures. Below 165°K  $\gamma$  satisfies condition (7.5) and below 160°K all  $\gamma$  values are so closely similar that one would be inclined to accept our alternative model. However, at the higher temperatures this model gives unacceptable results.

Table III  
Charge carrier concentrations (in  $\text{cm}^{-3}$ ) and mobilities (in  $\text{cm}^2/\text{V} \cdot \text{sec}.$ ) as computed at the various temperatures of the measurements

$T^\circ \text{K}$	125.6	138.5	146.3	151.5	156.8	159.4	162.0	164.7	167.3	172.5	177.8	188.5	204.5
$n_1 \cdot 10^{-13}$	-0.00435	-0.0637	-0.200	-0.472	-1.59	-1.63	-2.68	-3.47	-4.32	-7.01	-11.24	-26.9	-101
$n_2 \cdot 10^{-13}$	+65.44	+66.24	+66.57	+67.5	+68.8	+67.6	+72.0	+70.4	+70.98	+73.7	+78.21	+93.7	+169
$n_3 \cdot 10^{-13}$	+1.06	+0.282	+0.116	-0.217	-0.677	0.0845	-0.551	-0.356	-0.186	-0.181	-0.474	-0.235	-2.0
$b_1 \cdot 10^{-3}$	-92.77	-91.73	-90.76	-95.85	-66.79	-88.85	-75.99	-78.33	-84.40	-86.80	-85.69	-87.76	-66.84
$b_2 \cdot 10^{-3}$	+2.182	+2.060	+2.020	+2.115	+2.386	+1.932	+1.992	+1.815	+1.666	+1.661	+2.028	+1.685	+1.547
$b_3 \cdot 10^{-3}$	+16.93	+23.73	+33.13	+42.24	+66.62	+101.6	+59.61	+86.74	+110.3	+128.5	+101.15	+178.1	+237.2
$\frac{-n_1(n_2+n_3)}{T^3 \cdot 10^{+20}}$	0.146	1.60	4.25	9.09	27.8	27.2	44.9	54.4	61.9	101	155	376	1,980

Table IV  
Parameters of the alternative model

$T^\circ \text{K}$	125.6	138.5	146.3	151.5	156.8	159.4	162.0	164.7	167.3	172.5	177.8	188.5	204.5
$A(0)$	-7.124	-105.1	-7.351	-2.968	-1.377	-1.052	-0.8051	-1.080	-0.8485	-0.8587	-0.7173	-4.881	-4.639
$A(\infty)$	-3.095	-37.33	-5.525	-2.428	-1.164	-0.9188	-0.5832	-0.4173	-0.2891	-0.1702	-0.1094	-0.0458	-0.0177
$\gamma(\alpha = 1)$	1.057	1.074	1.050	1.060	1.080	1.073	1.218	1.796	2.091	3.305	4.476	25.0	82.8
$\gamma(\alpha = .849)$	1.074	1.068	1.043	1.056	1.074	1.066	1.209	1.783	2.073	3.284	4.395	24.7	80.4
$\gamma(\alpha = .5)$	1.162	1.041	1.015	1.034	1.048	1.035	1.169	1.728	1.991	3.092	4.056	23.4	71.1

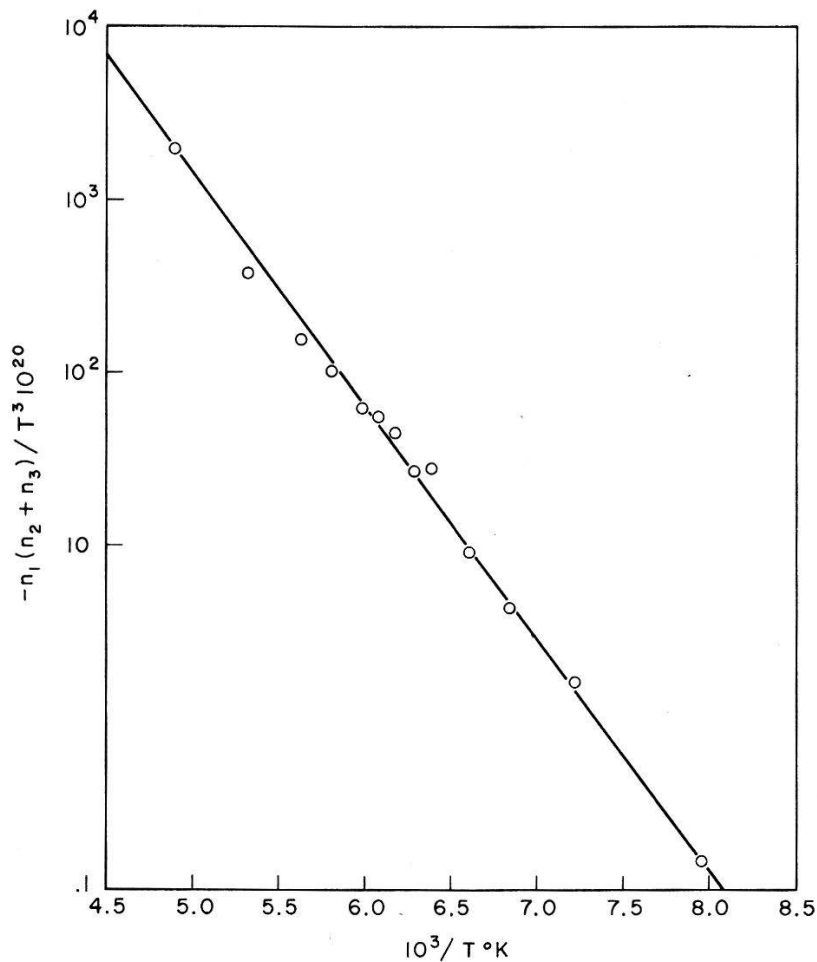


Fig. 13

Graph of  $\log [-n_1(n_2 + n_3)]/T^3$  versus  $1/T$ . The straight line has a slope which can be identified with  $-\Delta E/kT$ , yielding for the energy gap  $\Delta E = 0.27$  eV ( $k =$  BOLTZMANN constant)

### 8. Conclusions

The two models considered in this paper appear equally well suited to explain the properties of *p*-type InSb in the extrinsic range, but they both fail in the intrinsic range. In view of a great amount of evidence from other sources the three-band model is more likely to correspond to the facts. The analysis carried out here gives detailed information about the concentrations and mobilities of the different charge carriers. In the intrinsic range EHRENREICH<sup>5)</sup> has shown that the three band model can be maintained provided polar scattering is considered as the dominant mechanism determining the mobility of the electrons.

### 9. Acknowledgements

We wish to express our thanks to Dr. D. K. C. MACDONALD for his unfailing encouragement, to Drs. D. GREIG and J. S. DUGDALE for reading the manuscript, and Mr. ANDREW KORSACK for his assistance with the calculations.



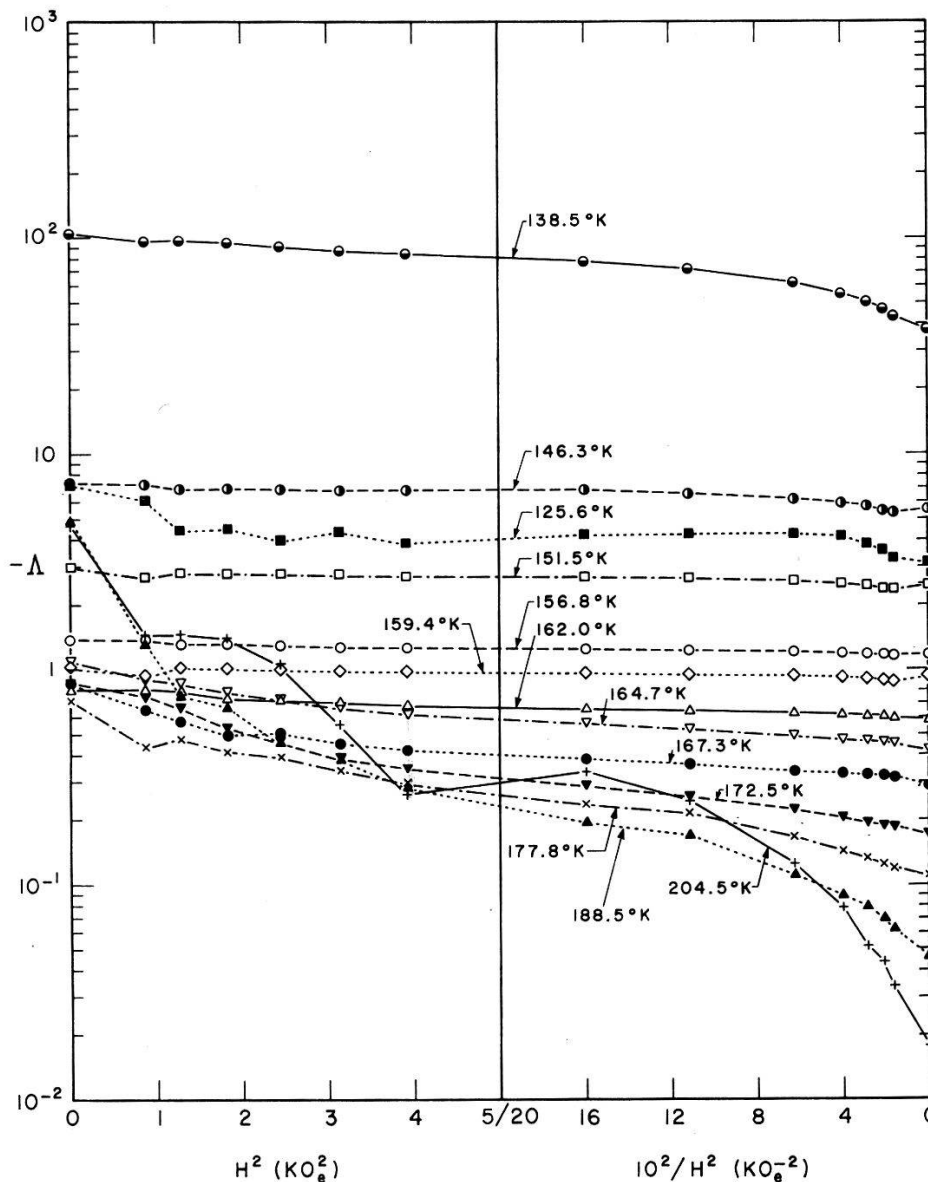


Fig. 14

Field and temperature dependence of the function  $A$  defined by (3.21). The points at  $H = 0$  and  $\infty$  are calculated with the help of Table II; all other points are experimental

**Appendix:**

**Solution of the Equations (2.13) to (2.20)\*)**

The three mobilities  $b_i$  are obtained as solutions of a cubic equation

$$b^3 - \alpha b^2 + \beta b - \gamma = 0 \tag{A.1}$$

where  $\alpha$ ,  $\beta$  and  $\gamma$  are simple function of the mobilities.

$$\alpha = b_1 + b_2 + b_3 \tag{A.2}$$

\*) The mathematical expressions of this solution have been worked out by Mr. Andrew Korsak, to whom we are very much indebted.

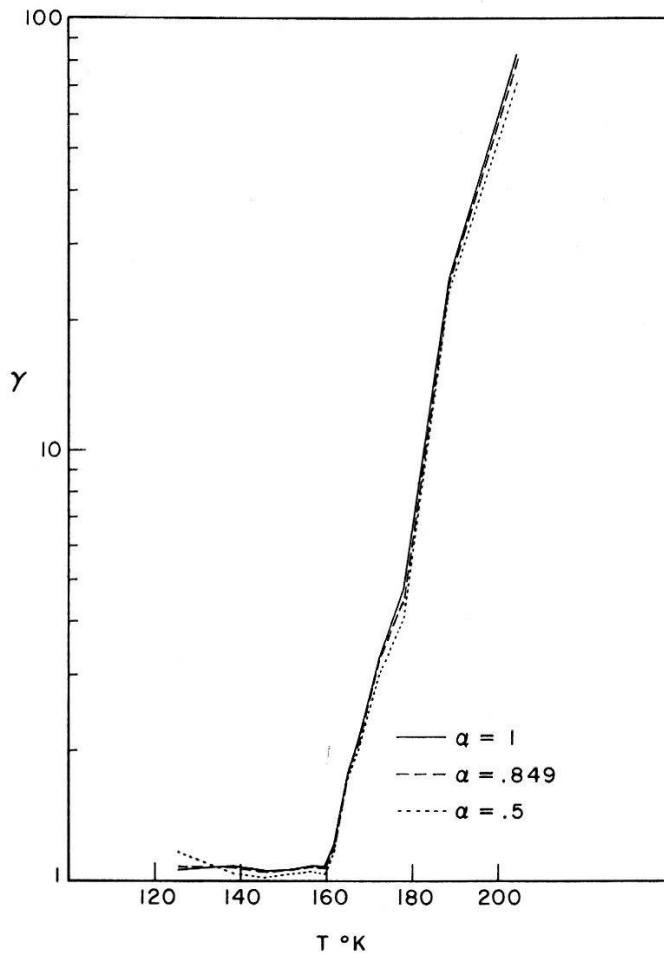


Fig. 15

Temperature dependence of parameter  $\gamma$  discussed in the alternative model (cf. section 7)

$$\beta = b_1 b_2 + b_2 b_3 + b_3 b_1 \quad (\text{A.3})$$

$$\gamma = b_1 b_2 b_3 \quad (\text{A.4})$$

$\alpha$ ,  $\beta$  and  $\gamma$  can be expressed in terms of the experimental parameters  $A$  to  $N$  appearing in (2.11) and (2.12). Since we have eight non-independent parameters, these expressions are not unique. We shall give here expressions which do not involve  $B$  and  $L$ .

$$\gamma = \frac{N}{\sqrt{M}} \quad (\text{A.5})$$

$$\alpha = \frac{1}{A} \left( E \pm \sqrt{D + 2A\sqrt{M}} \right) \quad (\text{A.6})$$

$$\beta = \frac{F - \gamma A + \alpha \sqrt{M}}{\alpha A - E} \quad (\text{A.7})$$

It is important to note that with our model, and with  $p$ -type InSb,  $\sqrt{M}$  is a negative number – cf. eqs. (2.17) and (2.24). Therefore  $\gamma$  is also

a negative number. It can also be shown that  $\alpha A - E$  is negative at low temperatures and positive at high temperatures; as a result the sign in front of the main root in (A.6) is not known a priori. A diagram of the positive values of this root exhibits a very well defined minimum at about 155°K. This minimum comes close to zero, and since we expect  $\alpha A - E$  to have a slowly changing derivative we assume the change of sign to occur at that temperature. Introducing the values obtained for  $\alpha$ ,  $\beta$  and  $\gamma$  into (A.1) gives an equation which always has a large negative root, attributed to  $b_1$ , and small and large positive roots, attributed to  $b_2$  and  $b_3$  respectively.

The charge carrier concentrations,  $n_i$ , can easily be expressed in terms of the mobilities,  $b_i$ , when solving the following set of equations:

$$n_1 + n_2 + n_3 = \frac{M}{N} \quad (\text{A.8})$$

$$n_1 b_1 + n_2 b_2 + n_3 b_3 = A \quad (\text{A.9})$$

$$n_1 b_1^2 + n_2 b_2^2 + n_3 b_3^2 = E \quad (\text{A.10})$$

and the solution is

$$n_1 = \frac{E - A(b_2 + b_3) + \frac{M}{N} b_2 b_3}{(b_1 - b_2)(b_1 - b_3)} \quad (\text{A.11})$$

with similar formulae for  $n_2$  and  $n_3$ .

### References

- 1) G. DRESSELHAUS, A. F. KIP, C. KITTEL, and G. WAGONER, *Phys. Rev.* **98**, 556 (1955).
- 2) H. P. R. FREDERIKSE and W. R. HOSLER, *Phys. Rev.* **108**, 1146 (1957).
- 3) E. O. KANE, *J. Phys. Chem. Solids* **7**, 249 (1957).
- 4) A. H. WILSON, *The Theory of Metals*, 2nd edition. Cambridge University Press (1953), p. 235.
- 5) H. EHRENREICH, *J. Phys. Chem. Solids* **2**, 131 (1957); **9**, 129 (1959).
- 6) R. K. WILLARDSON, T. C. HARMAN, and A. C. BEER, *Phys. Rev.* **96**, 1512 (1954).
- 7) A. C. BEER, *J. Phys. Chem. Solids* **8**, 507 (1959).
- 8) A. C. BEER and R. K. WILLARDSON, *Phys. Rev.* **110**, 1286 (1958).
- 9) G. FISCHER and D. K. C. MACDONALD, *Can. J. Phys.* **36**, 527 (1958).
- 10) H. J. LIPPMAN and F. KUHRT, *Z. Naturforschung* **13a**, 462 and 474 (1958).
- 11) C. HERRING, to be published, cf. ref. <sup>15</sup>, p. 1138.
- 12) R. C. CHAMBERS, *Proc. Phys. Soc. (London)* **A 65**, 903 (1952).
- 13) G. FISCHER and D. K. C. MACDONALD, *Phil. Mag.* **2**, 1393 (1957).
- 14) H. J. HROSTOWSKI, F. J. MORIN, T. H. GEBALLE, and G. H. WHEATLEY, *Phys. Rev.* **100**, 1672 (1955).
- 15) D. J. HOWARTH, R. H. JONES, and E. H. PUTLEY, *Proc. Phys. Soc. (London)*, **B 70**, 124 (1957).
- 16) H. P. R. FREDERIKSE and W. R. HOSLER, *Phys. Rev.* **108**, 1136 (1957).
- 17) R. T. BATE, R. K. WILLARDSON, and A. C. BEER, *J. Phys. Chem. Solids* **9**, 119 (1959).
- 18) O. G. FOLBERT, *Z. Naturforschung* **13a**, 856 (1958).